Journal of Molecular Graphics and Modelling 28 (2010) 487–494

Contents lists available at ScienceDirect

Journal of Molecular Graphics and Modelling

journal homepage: www.elsevier.com/locate/JMGM

Structural stabilization of a rigid β-sheet cluster of fucosylated proteinase inhibitor PMPC (*Pars intercerebralis* major peptide C) against thermal denaturation: An unfolding molecular dynamics simulation study

Youngjin Choi [a], Hyunmyung Kim [b], Jong Hyun Lee [c], Sungjun Park [d], Karpjoo Jeong [b], Seunho Jung [e,*]

[a] *BioChip Research Center, Hoseo University, Asan 336-795, Republic of Korea*
[b] *College of Information and Communication & Department of Advanced Technology Fusion, Konkuk University, Seoul 143-701, Republic of Korea*
[c] *Department of Computer Science, Konkuk University, Seoul 143-701, Republic of Korea*
[d] *Department of Game Engineering, Hoseo University, Asan 336-795, Republic of Korea*
[e] *Department of Bioscience and Biotechnology, Bio/Molecular Informatics Center, Konkuk University, 1 Hwayang-dong Gwangjin-gu, Seoul 143-701, Republic of Korea*

ARTICLE INFO

Article history:
Received 10 September 2009
Received in revised form 20 November 2009
Accepted 24 November 2009
Available online 3 December 2009

Keywords:
Conformational analysis
Non-local interaction
Glycosylation
Fucose
Denatured conformation
Unfolding MD simulations

ABSTRACT

Unfolding behavior of glycosylated- and unglycosylated proteinase inhibitor *Pars intercerebralis* major peptide C (PMPC) at 350 K were traced with molecular dynamics simulations using the CHARMM program. The fucosylated PMPC (FPMPC) possesses a nearly identical protein structure with PMPC, differing only by the presence of a single fucose residue linked to Thr9 in the PMPC. Attachment of a monomeric fucose residue to the Thr9 in PMPC resulted in a change of the denaturing process of FPMPC. Simulations showed that the unfolding of PMPC involved significant weakening of non-local interactions whereas fucosylation led FPMPC to preserve the non-local interactions, even in its denatured form. Even in simulations over 16 ns at 350 K, FPMPC remained relatively stable in a less denatured conformation. However, the conformation of PMPC transformed to a fully unfolded state within 5 ns in the simulation at 350 K. This difference was due to the formation of fucose-mediated hydrogen bonds and non-local contacts by the attached fucose residue of FPMPC. In the case of FPMPC, fucosyl residue was involved in maintaining a rigid β-sheet cluster through interaction with the hydrogen bond network. These high-temperature unfolding MD simulations provide a theoretical basis for a previous experimental work in which FPMPC showed stable unfolding thermodynamics compared to unfucosylated PMPC, suggesting that single fucosylation induces conformational stabilization of PMPC by tertiary contacts.

1. Introduction

Protein glycosylations are involved in a wide range of biochemical processes, including folding, cellular adhesion, immunity, and molecular stability of the protein families [1]. The biological glycosylation process consists of various kinds of glycan moieties, including the well characterized *N*- and *O*-glycosylation, both of which are potent effectors of many molecular phenomenons such as macromolecular recognition, conformation, and stability. Such modification is also critical for numerous biopharmaceutical applications including recombinant proteins, protein-drugs, and therapeutic glycoconjugates [2]. Carbohydrate chains in general, unlike amino acids and nucleic acid polymers, are assembled enzymatically without a defined template, and hence are diverse with respect to both the number and linkage patterns of the sugar units. Due to the heterogeneous nature of protein glycosylation both *in vivo* and *in vitro*, a comprehensive analysis of its effect on thermal stability has thus far proved elusive. However, studies of the stability of several unglycosylated proteins in the presence of high concentrations of saccharides have led to the conclusion that glycans stabilize folded proteins due to preferential interaction with the native state through hydrogen bonds as well as water trapping or entrapment of a particular protein conformation in a viscous sugar-glass [3,4]. Such observations provide some indication that glycosylation of native proteins could induce a microenvironment similar to that of unmodified proteins in sugar solutions [5].

It has long been established that protein glycosylation stabilizes the native conformations of many proteins against thermal denaturation. However, the molecular basis for the glycosylation effects upon conformational stabilization was poorly understood. It is highly important to gain insight into the dynamic effects of glycosylation on the conformation of protein molecules. Even though such conformational effects are not the sole function of glycosylation for biological proteins, glycosylated proteins with an identical structure to unglycosylated proteins may provide

* Corresponding author. Tel.: +82 2 450 3520; fax: +82 2 452 3611.
E-mail address: shjung@konkuk.ac.kr (S. Jung).

1093-3263/$ – see front matter © 2009 Elsevier Inc. All rights reserved.
doi:10.1016/j.jmgm.2009.11.003

valuable insight into the stabilization mechanism. In this study, *L*-fucosylated protein was used as an *in silico* model of a glycoprotein to mimic the conformational effect of glyco-moiety on the protein structure and dynamics. Comparative unfolding molecular simulations [6] were performed to evaluate the dynamics and stability of the proteinase inhibitor PMPC (*Pars intercerebralis* major peptide C) and fucosylated PMPC (FPMPC).

Experimental results presented by Mer et al. [7] motivated further experimental and theoretical studies to establish a link between fucosylation of PMPC and the protein dynamics/stability. They found that overall backbone conformations of nonfucosylated PMPC and fucosylated one on Thr9 were very similar and could not be discriminated from one another. However, just mono-fucosylation increased the overall thermal stability of PMPC in the high-temperature of denaturing condition. They measured the thermodynamic stability of PMPC fucosylated on Thr9 via a NMR analysis. The exchange rates of amide protons measured by the NMR spectroscopy indicated that mono-fucosylation was responsible for an overall decrease of the dynamic fluctuations of the FPMPC. This correlated well with an increase in stability of ~1 kcal/mol, as monitored by thermal denaturation. Therefore, it is important to establish a factor to contribute overall thermal stability by mono-fucosylation upon denaturing condition rather than native structure.

In this study, we report on the conformational stabilities of single fucosylated- and unfucosylated-PMPC in the denaturing condition from results of high-temperature molecular dynamics (MD) simulations along with a comparison of findings of previous experiments. The model system of glycosylation was constructed with monomeric *L*-fucose [7]. The solution conformations for PMPC and FPMPC were traced with 16 ns molecular dynamics simulations using the CHARMM [8] program at a 350 K unfolding temperature for the PMPC. This unfolding simulation approach has previously been successfully employed to explain the folding/unfolding process of some proteins [9–11]. With the MD approach, we found that fucosylation increased the structural rigidity of the β-sheet core of PMPC at a high-temperature of 350 K. The formation of stable secondary and tertiary structures in proteins is dictated by intra-molecular interactions between the constituent amino acid residues along the polypeptide chain. Each amino acid residue is assembled in a compact and dense atomic structure that interacts with other residues via short-range or long-range interactions. In the case of FPMPC, fucosyl residue is involved through bridged hydrogen bonds in maintaining both secondary and tertiary structure.

2. Methodology

2.1. Protein structure and molecular model

The starting 3D structure of PMPC was obtained from the NMR structure in Protein Data Bank (PDB id 1PMP). The fucosylated form of PMPC (FPMPC) was made by modification at the Thr-9 residue from the 3D coordinates of PMPC. The three-dimensional PMPC structure is known to consist of three antiparallel β-sheets without α-helices. The overall conformation is arranged in a right-handed twisted antiparallel motif in which β-sheets demarcates a cavity together with a linear N-terminal segment oriented almost perpendicular to the three strands [7,12]. The β-sheets are composed of β1 (residues 8–11), β2 (residues 16–19), and β3 (residues 26–30). The overall backbone conformations of fucosylated and unfucosylated PMPC are known to be very similar and could not be distinguished from one another.

For the low-pH simulations, the ionization state of the charged residue was set to mimic the pH 3 solutions used in NMR experiments [7]. For this, positively charged His, Lys, and Arg residues, and protonated acidic groups were used. Schematic representations of the PMPC and FPMPC are summarized in Fig. 1. Six chlorine counter ions were added to maintain electric neutrality of the system. The geometries of these molecular models were fully energy-minimized before MD runs.

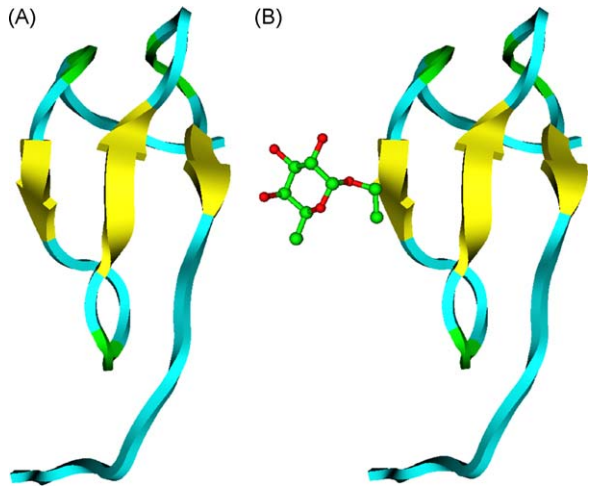

Fig. 1. Schematic representations of (A) PMPC and (B) FPMPC studied in this work. The secondary structure was assigned by the Kabsch & Sander method. The *L*-fucose residue of FPMPC was rendered by a ball and stick model. The figure was drawn with MOE program.

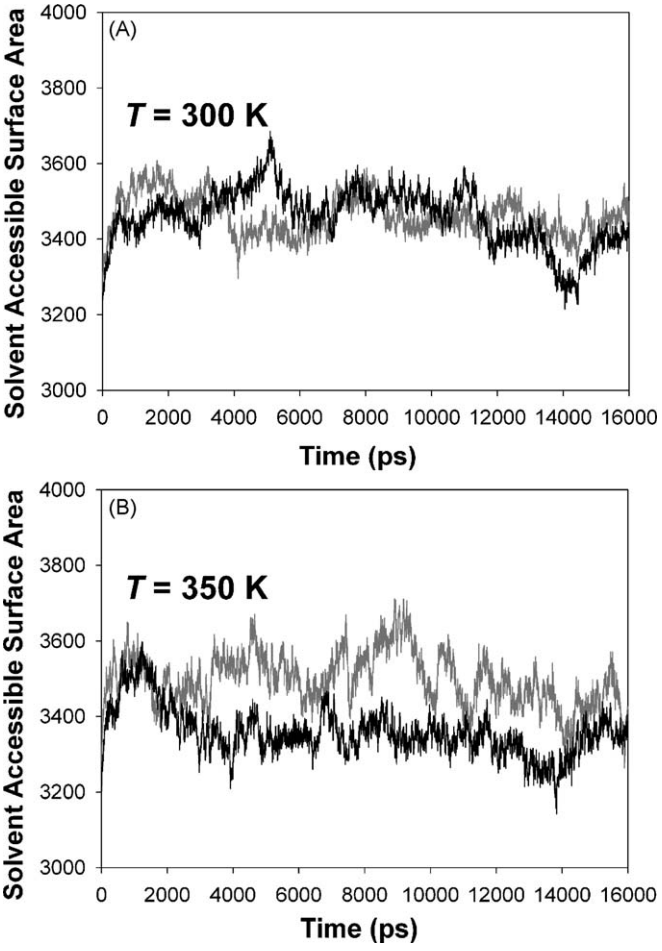

Fig. 2. Time evolution for the increase of solvent-accessible surface area (SASA) of the PMPC (gray line) and FPMPC (black line) at 300 K (A) and 350 K (B) during MD simulations. The SASA difference between PMPC and FPMPC was more significant at 350 K of high-temperature MD simulation.

2.2. Unfolding molecular dynamics simulation and trajectory analysis

The unfolding MD simulations were performed using the CHARMM 31b1 program in the isothermal-isobaric ensemble (P = 1 bar, T = 350 K). An all-atom CHARMM22 force field was used to calculate the dynamics of protein parts of the PMPC. The remaining sugar moiety was parameterized with a carbohydrate solution force field [13] for the CHARMM program. Control simulations were performed at 300 K to mimic the temperature condition below the melting points of both PMPC and FPMPC [7]. Ten unfolding simulations were performed at 350 K with different random number seeds. A TIP3P three-site rigid water model [14] was used to solvate each PMPC or FPMPC. Water molecules were removed if they were closer than 2.8 Å to any heavy atoms of the proteins. In summary, each system was constructed using periodic boundary conditions with a cubic box of dimensions 50 Å × 50 Å × 50 Å, consisting of the protein and water molecules. The system was minimized by 1000 steps of conjugate gradient, followed by Adopted Basis Newton–Raphson until the root-mean-square gradient was less than 0.001 kcal/mol. The particle mesh Ewald summation method [15] was used to treat the long-range electrostatic interactions. The number of grid points for the charge mesh and the kappa value were chosen to be 54 and 0.347, respectively. The bond lengths of water and each PMPC were constrained with the SHAKE algorithm [16]. The time step was 2.0 fs, and the non-bonded pair list was updated every 25 steps. Lennard–Jones interactions were truncated from 13- to 8-Å with a switching function in the CHARMM program. The temperature and pressure of the system was regulated using the Langevin piston method in conjunction with Hoover's thermostat [17]. The system was gradually heated to 350 K for 50 ps and equilibrated for 500 ps at this temperature. The production MD trajectory with one snapshot per 4 ps was collected for 16 ns. All the dynamic simulations were performed on a computing system of the Applied Grid Computing Center in Konkuk University. Final MD trajectories were analyzed and processed using a computational grid system, called MGrid (http://www.mgrid.or.kr), to process a large number of MM calculations simultaneously. The MGrid system was designed to support remote execution, file sharing, and standard web-interface to molecular simulation software so as to run successful MD simulations.

The close contacts and other geometric elements were computed using the analysis facility of the CHARMM program. Close contact was defined based on a cutoff distance of 6 Å between any C_α atoms. A native contact in NMR structure was defined as a contact between any two non-sequential C_α atoms

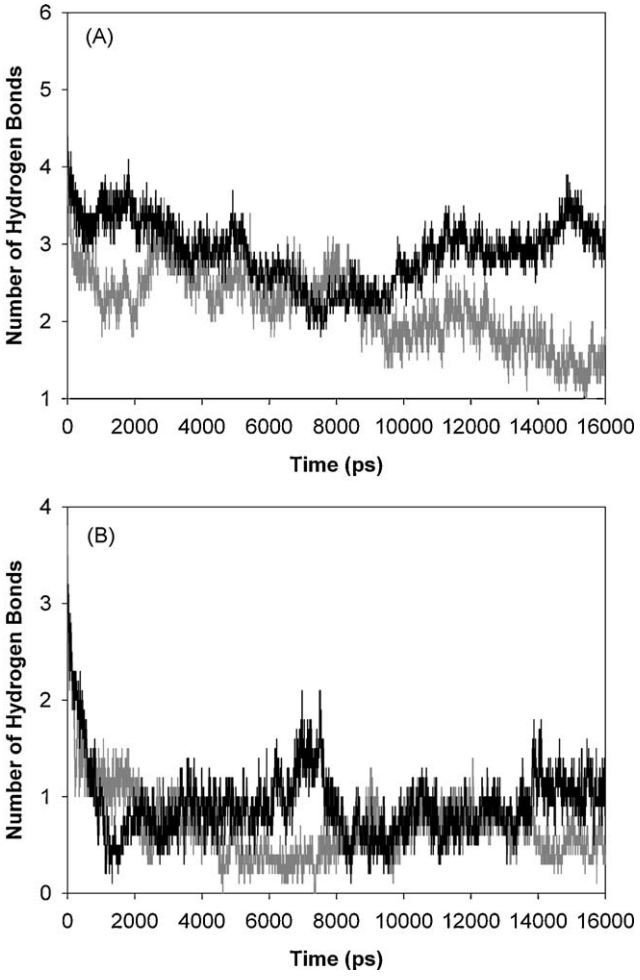

Fig. 3. Time evolution for the number of hydrogen bonds between β-strands of the PMPC (gray line) and FPMPC (black line) at 350 K. (A) Number of hydrogen bonds between β1 and β2; (B) number of hydrogen bonds between β2 and β3. The hydrogen bond was defined to exist when the donor H to acceptor atom distance was less than 3 Å and the angle was higher than 120° from linear.

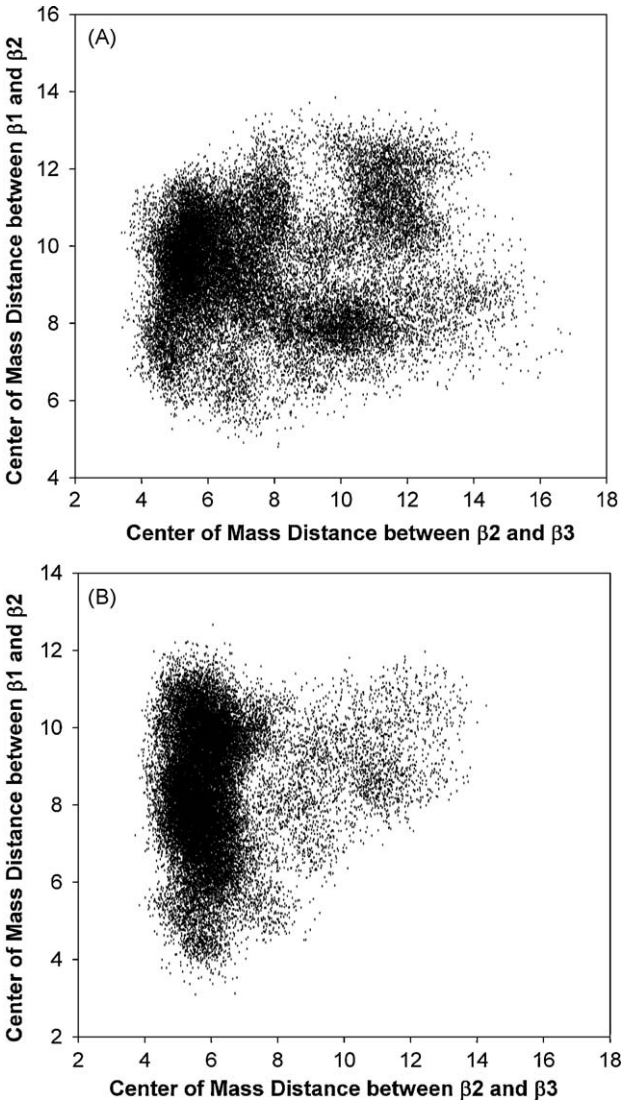

Fig. 4. 2D scatter plots for the center of mass distance between β1/β2 and between β2/β3 for the PMPC (A) and FPMPC (B). This 2D map shows a relatively homogeneous conformation of FPMPC at denaturing condition compared to disordered structure of PMPC.

with an inter-atomic distance of <5.5 Å. For the unfolding MD simulations, the native contacts were counted if the inter-atomic distance was maintained within 6 Å to allow a temporary fluctuation. A non-local contact was defined as close contacts between residue i and j in the protein in which $i + j$ are above 5 ($|i - j| > 5$).

3. Results and discussion

3.1. Differences in conformational stabilities of PMPC and FPMPC during MD simulations

The unfolding process is known to be stochastic and the trajectories vary from each other. Multiple trajectory simulations were carried out at 350 K to reduce statistical error. Ten different unfolding simulations were performed and all computational results including the number of hydrogen bonds here are numerical mean values over the trajectory files. Number of hydrogen bonds per residue in the time course for PMPC and FPMPC are shown in Supplementary Fig. 1 as an averaged value. PMPC and FPMPC showed similar decreasing patterns for the number of hydrogen bonds per residue. Averaged values during the stable late 10 ns of MD simulations were 0.62 and 0.71 for PMPC and FPMPC, respectively. This indicates that FPMPC possesses a stable tertiary structure compared with PMPC in the MD time scale, suggesting that fucosylation in FPMPC may preserve the structural rigidity of the protein during high-temperature MD simulations.

The progress of each MD simulation was also monitored on the basis of solvent-accessible surface area (SASA) changes in order to compare conformational stabilities. The time evolutions of a SASA at 350 K for PMPC and FPMPC are shown in Fig. 2B. During the early unfolding process (T = 350 K), a rapid increase of SASA was observed for the PMPC, indicating a tendency toward conformational destabilization. The averaged SASA value was recorded as 3491 and 3338 Å^2 for PMPC and FPMPC, respectively. The SASA value was decreased by about 5% due to the fucose residue of FPMPC. This indicates that fucosylation increased the conformational stability of FPMPC during the MD time scale. The SASA data from the unfolding MD simulation (T = 350 K) was comparable with that of the control MD simulation at 300 K (Fig. 2A). The SASA change during MD simulations was almost identical for the PMPC and FPMPC. The averaged SASA difference between PMPC and FPMPC was only 0.3% at the 300 K MD simulations. Conformational stabilization by the fusosyl residue may not be very effective for a native structure of PMPC at 300 K. The denatured conformations

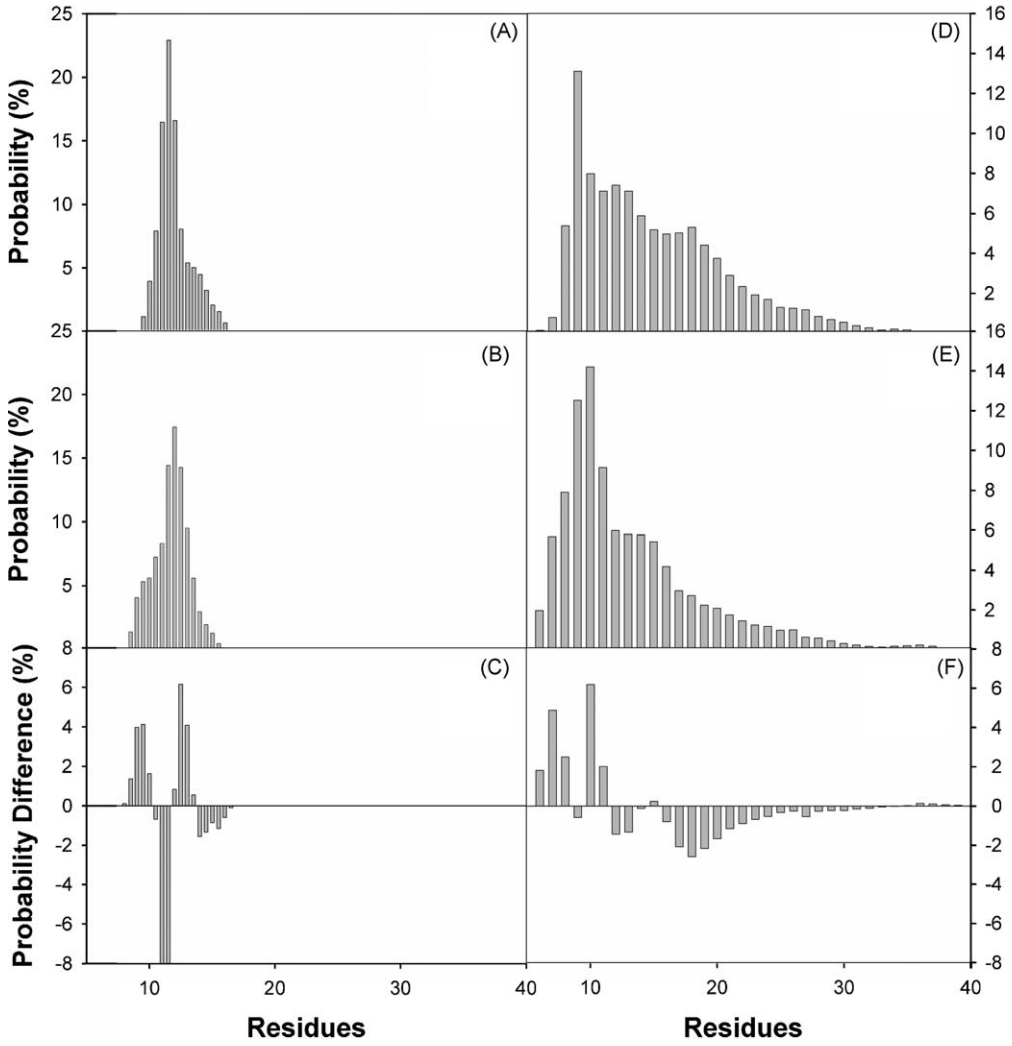

Fig. 5. Probability distribution for the center of mass distance between β1 and β3 of the PMPC at 300 K (A), FPMPC at 300 K (B), probability difference between PMPC and FPMPC at 300 K (C), PMPC at 350 K (D), FPMPC at 350 K (E), and probability difference between PMPC and FPMPC at 350 K (F). The FPMPC showed more rigid conformational feature as compared to PMPC at 350 K.

traced by hydrogen bonding and SASA value are further discussed in the following sections.

3.2. Conformational stabilization by inter-strand interaction in the FPMPC

It is of interest to compare in greater detail the average interatomic hydrogen bonds between β-strands so as to observe the fucosylation effect. Total hydrogen bonds for β1–β2 and β2–β3 are compared in Fig. 3. For the hydrogen bonds between β1 and β2, FPMPC showed stable inter-strand hydrogen bonds. Averaged values during the production phase of the MD simulations were 1.98 and 2.76 for PMPC and FPMPC, respectively (Fig. 3A). Moreover, a significant increase in hydrogen bonds for FPMPC was observed during the late phase of the unfolding simulations after 10 ns. In the case of interaction between β2 and β3, FPMPC was also characterized by hydrogen bonds showing an average value of 0.59 and 0.90 for PMPC and FPMPC, respectively (Fig. 3B). However, the absolute number of inter-strand hydrogen bonds between β2 and β3 was lower than the number of hydrogen bonds between β1 and β2 for both PMPC and FPMPC. The fucosylation at β1 appears to mainly affect conformational stability around the inter-strand region between β1 and β2 rather than for the region between β2 and β3.

Fig. 4 is the center of mass distance between β-strands in the PMPC and FPMPC during the MD simulations. The 2D maps for the distance between β1–β2 and between β2–β3 represent conformational characteristics of PMPC and FPMPC. For the PMPC, the averaged distance for the β1/β2 and β2/β3 pair was 7.69 and 9.41 Å, respectively. The β1/β2 pairing showed relatively strong interaction for the β-strands. In the case of FPMPC, the distance was 6.15 and 8.38 Å for the β1/β2 and β2/β3 pair, respectively. Distributions for the center of mass distance of PMCP and FPMPC are a distinguished feature for conformational stabilization by fucosylation. The heterogeneous distribution observed in the PMPC reflects that PMPC underwent an order–disorder conformation changes during high-temperature MD simulations. However, the FPMPC showed a relatively homogenous feature for the 2D-distance distribution, especially for the β2/β3 pairing. The shorter distance of β1/β2 for the FPMPC may be affected by the fucose residue attached to the Thr9 of the protein.

The differences in inter-strand interaction between PMPC and FPMPC were compared in terms of structural rigidity. Analogous to experimental protein unfolding, the loss of rigidity in a certain region is considered to precede the order–disorder transition from a more rigid to a more flexible state of the protein structure [18,19]. Therefore, the folded to unfolded transitions in the proteins can be regarded as a rigid to flexible transition per residue. Both PMPC and FPMPC are composed of three rigid β-strands in their core structure. This rigid cluster can be verified as a sharp distribution of center of mass distance between β1 and β3 at 300 K (Fig. 5A, B). The distance distribution of the rigid cluster did not vary during the 300 K MD simulations for both PMPC and FPMPC, showing an average value of ca. 13 Å. However, this rigid clustering was disrupted during the 350 K unfolding MD simulations for both PMPC and FPMPC (Fig. 5D, E). The transition toward disordering in the protein is observed as a disruption of the hydrogen bond network [20]. Hence, the rigid β-strand cluster is changed to an expanded and flexible state accompanied by a heterogeneous distribution of the distance between β1 and β3. In particular, FPMPC showed a relatively rigid conformation (shorter distance) as compared to PMPC at 350 K (Fig. 5D–F). The positive values in the probability difference indicate that FPMPC has more conformational status at the corresponding shorter inter-strand distance. The probability difference results (Fig. 5F) indicate FPMPC maintains a more rigid conformation at 350 K whereas the conformational difference between FPMPC and PMPC is negligible at 300 K. These results are evidence that fucose residue enhanced the rigidity of FPMPC by backbone interaction at the high-temperature of 350 K.

The C_α contact maps of PMPC and FPMPC were compared in order to establish the stability of the backbone structures (Fig. 6). Only long-term contacts with life-time higher than 500 ps were considered to exclude the effect of temporal structure organization. Total occurrence number of C_α contacts of each PMPC and FPMPC was 73 and 145, respectively. A two-fold increase in long-term contacts reflects the higher backbone stability of FPMPC. Moreover, PMPC showed local inter-strand contact between β1 and β2 or between β2 and β3 (Fig. 6A). There were no remote contacts between β1 and β3 for the case of PMPC. For the case of FPMPC, stable contacts between β1 and β3 were observed as well as contacts between β1 and β2 or between β2 and β3 (Fig. 6B). Overall analyzed data indicate fucosyl residue reinforce backbone stability of FPMPC by mediated inter-strand interactions, rather than solely by fortification of local molecular interactions.

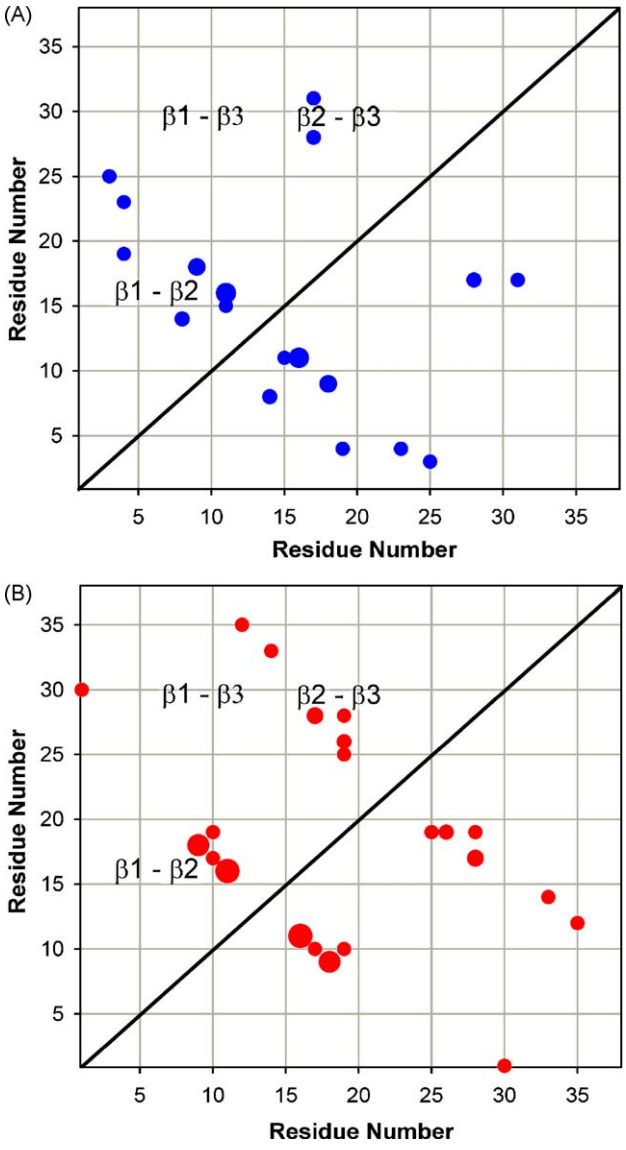

Fig. 6. Residue–residue C_α contact maps for the overall conformations of PMPC (A) and FPMPC (B) during MD simulations. The FPMPC showed stable long-rang contacts between β1 and β3.

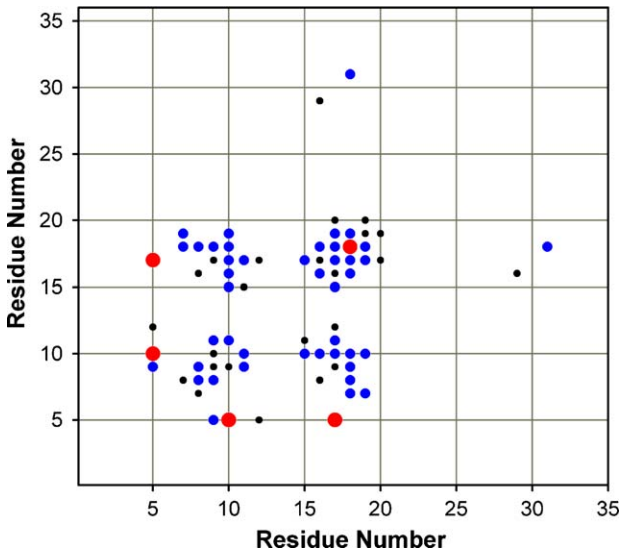

Fig. 7. Hydrogen bond bridge formation of FPMPC via attached fucose residue during MD simulations at 350 K. Red, blue, and black filled circle represent strong, medium, and weak bridged hydrogen bonds with 500, 200, and 100 ps half-life time, respectively.

3.3. Unfolding retardation of FPMPC by non-local interactions mediated by single fucosyl residue

The single fucosyl residue mainly affected the denatured conformation of FPMPC, rather than the native structure. Computational data for the MD trajectories suggested a possibility of global effects on the denatured conformation of FPMPC by fucose in addition to local structural influences. The amino acid residues in FPMPC were in multiple contacts with the fucosyl sugar residue, even though the protein underwent denaturation. Fig. 7 shows hydrogen bond bridges between amino acid residues mediated by fucose in FPMPC at 350 K. A number of hydrogen bonds are formed between the protein atoms and single sugar residue in the denatured condition at 350 K. During the high-temperature MD simulations, the fucosyl residue formed many hydrogen bond bridges with various residues in FPMPC. In particular, Glu5/Phe10, Glu5/Cys17, and Cys17/Arg18 showed strong bridged hydrogen bonds with a 500 ps half-life time. Thus, the fucosyl residue mainly stabilizes the inter-strand interaction between β1 and β2. Moreover, Cys4, Lys8, Thr9, Lys11, Asn15, Thr16, and Lys31 acted as additional bridged hydrogen bond acceptors with a 200 ps half-life time, and these residues were involved β1, β2, and β3 interactions. These results indicate that the fucosyl residue mediates multiple contacts between β-strands in FPMPC using pertinent hydrogen bond bridges. Thus, fucosylation may mitigate the conformational denaturation process through the formation of multiple interactions via bridged hydrogen bonds with not only β1/β2 but also β2/β3 inter-strand interactions in FPMPC.

The protein unfolding process generally involves the transition of the backbone from an ordered to a disordered state and, therefore, hydrogen bonds or native contacts are broken as this process proceeds. In order to elucidate differences in the denaturing process of PMPC and FPMPC, native contacts and close contacts between C_α atoms were analyzed. As definition, total twenty native contacts were found in the NMR structure of PMPC. A list of the pertinent native contacts was summarized as a table in supplementary material. The changes of native contact percentage during the MD simulations at 350 K were shown in Fig. 8. To be defined as a native contact, the two non-sequential C_α atoms of the protein structures have to be within 6 Å of each other over the course of MD simulations. With the protein spread, the native

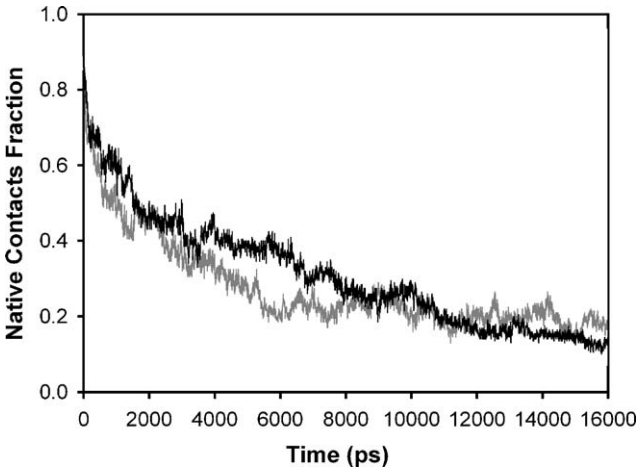

Fig. 8. Time evolution for the decrease of native contact fraction of the PMPC (gray line) and FPMPC (black line) at 350 K. Unfolding of FPMPC was relatively retarded by less disrupted native contacts in the initial phase of MD simulations.

contacts were decreased as shown in Fig. 8. During 3–7 ns of MD time scale, the native contact fraction was 0.27 and 0.37 for the PMPC and the FPMPC, respectively. Therefore, unfolding of FPMPC was relatively retarded by increasing native contact in the initial phase of MD simulations. However, both PMPC and FPMPC showed similar native contact fraction after 10 ns. The value was 0.19 and

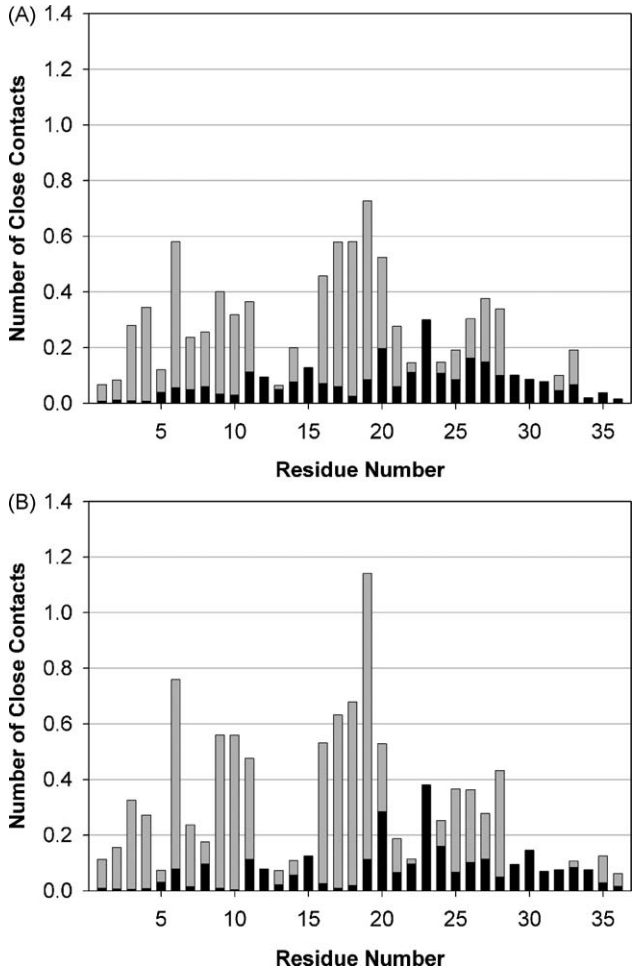

Fig. 9. Local (black bar) and non-local contact (gray bar) of the PMPC (A) and FPMPC (B) during MD simulations at 350 K. This data is indicative of structural reorganization of FPMPC by non-local contacts in its denaturing condition.

0.17 for the PMPC and the FPMP, respectively. That means just below 20% native contacts left over after 350 K of MD simulations from the initial structure. Hence, it was not significant how much native contact was discernable between PMPC and FPMPC during the unfolding MD simulations except initial phase of MD time scale.

Further analysis was performed for a total close contact to found additional index on thermal stability of FPMPC by fucosylation. The total close contact provides non-native contact information on the protein structure as well as native contact. A reduction in the number of total close contacts of PMPC and FPMPC during 350 K MD simulations could be found in Supplementary Fig. 2. The proteins lost their intermolecular stability from the native structure as the simulation process proceeded. The average fraction of close contacts of PMPC was changed from 1.0 to 0.65 and that of FPMPC from 1.0 to 0.67 during the last 10 ns of the simulation time period. This indicates that the close contacts were disrupted by about 35% during the MD simulations for both PMPC and FPMPC. The final level of close contacts for both proteins was quite similar. Therefore, this information on the native or close contacts disruption not enough to provide a clear reason as to why FPMPC showed a relatively stable conformation against 350 K unfolding conditions.

In order to obtain a detailed view of the close contacts of both PMPC and FPMPC, the contacts were divided into two categories, local and non-local interactions. The non-local contact was defined as close contacts between residue i and j in the protein in which $i + j$ are above 5 ($|i - j| > 5$). Fig. 9 presents the averaged contact number for each amino acid residue of PMPC and FPMPC. For the local contact, a slight difference was observed between PMPC and FPMPC, in which only Gly20 and Gly23 showed meaningful disparity between the proteins. However, significant discrepancies were estimated for the case of non-local contact. In particular, the non-local contact of Pro6, Phe10, Thr16, Cys19, and Cys28 was increased by about 30.9, 75.4, 16.4, 56.9, and 27.7%, respectively, when PMPC was modified by a single fucosyl residue on the Thr9 of PMPC. This is indicative of structural rearrangement of FPMPC in its denaturing conditions by non-local interactions between β1, β2, and β3 strands. The representative pictures during unfolding MD simulations for the structural stabilization mediated by fucose residue were obtainable in supplementary material.

3.4. Secondary and tertiary structural stabilization by the fucosyl residue in FPMPC

Protein secondary structure is an important index to judge conformational stability of a protein. The high-temperature of 350 K provides unfolding pressure for the PMPC protein, which will show decay of its secondary structure. Both PMPC and FPMPC maintain their secondary structures with the characterized β-strands at the 300 K simulation temperature (Supplementary Fig. 3). There were small changes in the secondary structure of both proteins; therefore, the conformational stabilities of the two proteins are almost identical. However, the 350 K MD temperature induced decay of the secondary structure (Fig. 10). For the case of PMPC, final disruption the secondary structure was found in 6-trajectories among the ten-multiple simulation trajectories (Fig. 10A). However, there was just one case of destabilization in the case of FPMPC (Fig. 10B). The secondary structure was clearly stabilized with only partial decay by a single fucosyl residue in FPMPC.

This secondary structural stabilization was correlated with the stable tertiary structure of FPMPC during the unfolding process. Fig. 11 is a probability-density map for the R_G-RMSD values of both PMPC and FPMPC. There were two main local minima in the denatured conformation for the case of PMPC along with an increased value of RMSD (Fig. 11A). This indicates PMPC is able to undergo conformational changes to a disordered form during the

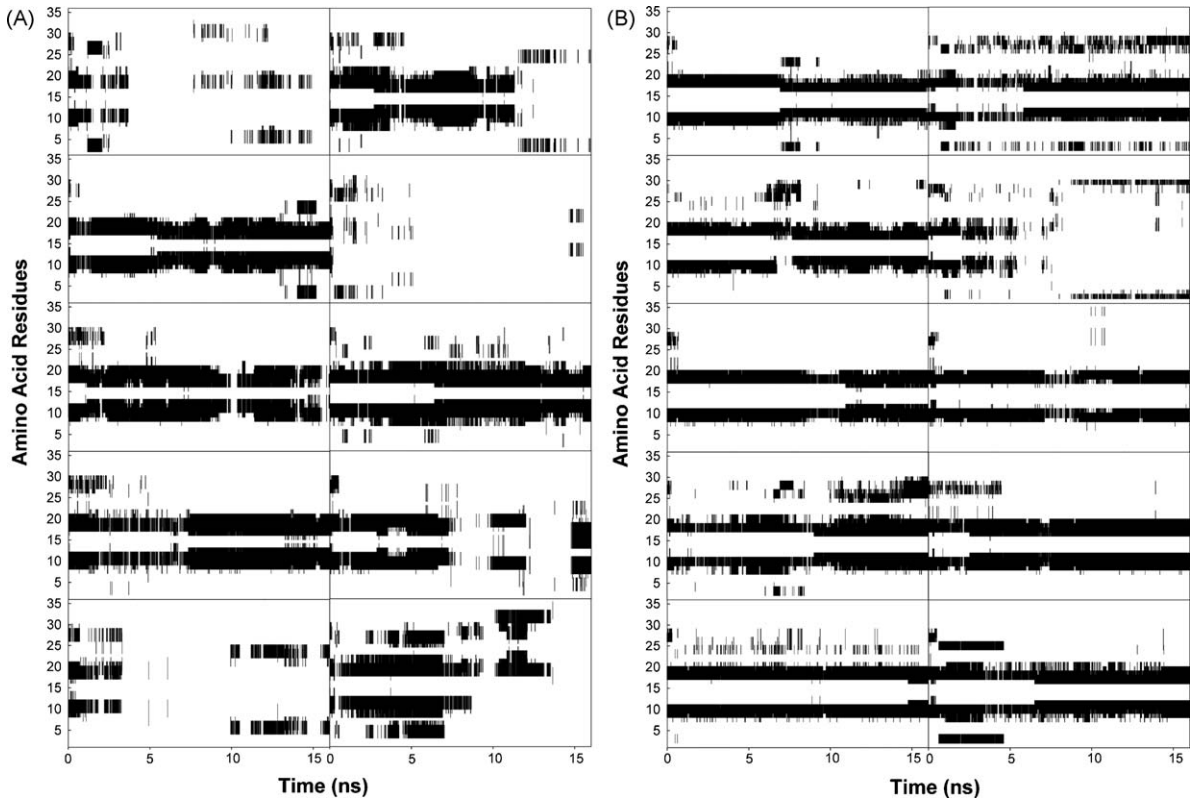

Fig. 10. Secondary structure changes of PMPC (A) and FPMPC (B) during MD simulations at 350 K. Only β-strands are shown in this figure and other secondary structures are omitted for clarity.

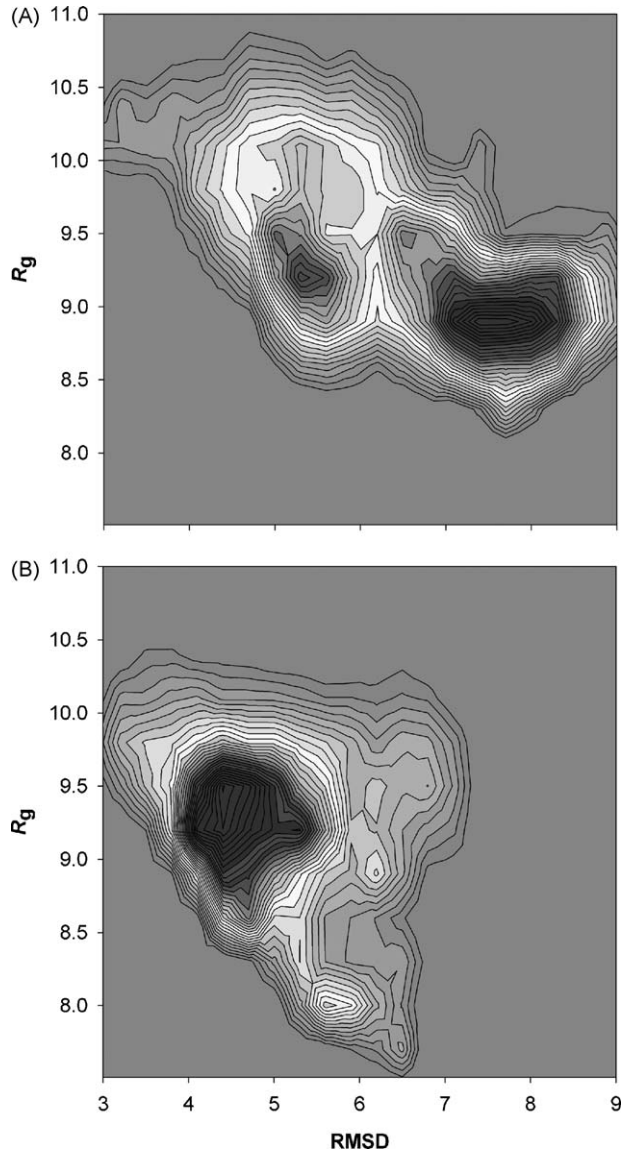

Fig. 11. Probability-density map for the distribution of R_G and RMSD for the PMPC (A) and FPMPC (B). The FPMPC maintains a rigid structural integrity in its denaturing condition.

unfolding conditions due to limited non-local interactions between amino acid residues. However, FPMPC showed only one global minimum in the denaturing conditions with little change of the RMSD value from the native conformation. As compared to PMPC, the structure of FPMPC maintains a relatively rigid state to hinder global ordered to disordered changes. Therefore, because of its single fucosyl residue, FPMPC was not readily denatured during 350 K MD simulations. This is direct evidence of tertiary structure stabilization of FPMPC by the attached fucosyl sugar residue.

4. Conclusions

Comparison of the dynamics of PMPC and FPMPC during unfolding simulations demonstrates that glycosylation affects the denatured conformation of the proteins even though the proteins only differ by one attached fucosylated residue. High-temperature multiple unfolding MD simulations of PMPC and FPMPC have provided important theoretical insight into the denatured conformational differences, suggesting that single fucosylation increased the stability of non-local interactions and thereby inhibits the formation of a highly random conformation during the unfolding process. FPMPC preserved more rigid β-strand clustering as compared to PMPC. The present study is an attempt to understand how single fucosylation changes the conformational characteristics of proteins during the denaturation process via unfolding MD simulations. Based on these simulations, we conclude that a single fucosyl sugar residue attached to PMPC can alone lead to overall structural stabilization of the denatured conformation of FPMPC, via fortification of the secondary and tertiary structure during unfolding process, far beyond the limited local effect.

Acknowledgement

This study was supported by National Research Foundation of Korea Grant funded by the Korean Government (2008-C00143).

Appendix A. Supplementary data

Supplementary data associated with this article can be found, in the online version, at doi:10.1016/j.jmgm.2009.11.003.

References

[1] C. Wang, M. Eufemi, C. Turano, A. Giartosio, Influence of the carbohydrate moiety on the stability of glycoproteins, Biochemisty 35 (1996) 7299–7307.
[2] A.M. Sinclair, S. Elliott, Glycoengineering: the effect of glycosylation on the properties of therapeutic proteins, J. Pharm. Sci. 94 (2005) 1626–1635.
[3] R.D. Lins, C.S. Pereira, P.H. Hunenberger, Trehalose–protein interaction in aqueous solution, Proteins 55 (2004) 177–186.
[4] G. Xie, S.N. Timasheff, Mechanism of the stabilization of ribonuclease a by sorbitol: preferential hydration is greater for the denatured than for the native protein, Protein Sci. 6 (1997) 211–221.
[5] R.S. Swanwick, A.M. Daines, L.H. Tey, S.L. Flitsch, R.K. Allemann, Increased thermal stability of site-selectively glycosylated dihydrofolate reductase, Chem. Bio. Chem. 6 (2005) 1338–1340.
[6] Y. Choi, J. Lee, S. Hwang, J.K. Kim, K. Jeong, S. Jung, Retardation of the unfolding process by single N-glycosylation of ribonuclease A based on molecular dynamics simulations, Biopolymers 89 (2008) 114–123.
[7] G. Mer, H. Hietter, J.F. Lefevre, Stabilization of proteins by glycosylation examined by NMR analysis of a fucosylated proteinase inhibitor, Nat. Struct. Biol. 3 (1996) 45.
[8] B.R. Brooks, R.E. Bruccoleri, B.D. Olafson, D.J. States, S. Swaminathan, M. Karplus, CHARMM: a program for macromolecular energy, minimization, and dynamics calculations, J. Comput. Chem. 4 (1983) 187–217.
[9] W. Gu, T. Wang, J. Zhu, Y. Shi, H. Liu, Molecular dynamics simulation of the unfolding of the human prion protein domain under low pH and high temperature conditions, Biophys. Chem. 104 (2003) 79–94.
[10] N.J. Marianayagam, S.E. Jackson, The folding pathway of ubiquitin from all-atom molecular dynamics simulations, Biophys. Chem. 111 (2004) 159–171.
[11] R. Day, B.J. Bennion, S. Ham, V. Daggett, Increasing temperature accelerates protein unfolding without changing the pathway of unfolding, J. Mol. Biol. 322 (2002) 189–203.
[12] G. Mer, H. Hietter, C. Kellenberger, M. Renatus, B. Luu, J.F. Lefevre, Solution structure of PMP-C: a new fold in the group of small serine proteinase inhibitors, J. Mol. Biol. 258 (1996) 158–171.
[13] K.J. Naidoo, M. Kuttel, Water structure about the dimer and hexamer repeat units of amylose from molecular dynamics computer simulations, J. Comput. Chem. 22 (2001) 445–456.
[14] W.L. Jorgensen, J. Chandrasekhar, J.D. Madura, R.W. Impey, M.L. Klein, Comparison of simple potential functions for simulating liquid water, J. Chem. Phys. 79 (1983) 926–935.
[15] T. Darden, D. York, L. Pedersen, Particle mesh Ewald: an N·log(N) method for Ewald sums in large systems, J. Chem. Phys. 98 (1993) 10089–10092.
[16] J.P. Ryckaert, G. Ciccotti, J.J.C. Berendsen, Numerical integration of the Cartesian equations of motion of a system with constraints: molecular dynamics of n-alkanes, J. Comput. Phys. 23 (1977) 327–341.
[17] S.E. Feller, Y. Zhang, R.W. Pastor, B.R. Brooks, Constant pressure molecular dynamics simulation: the Langevin piston method, J. Chem. Phys. 103 (1995) 4613–4621.
[18] V.G.H. Eijsink, A. Bjørk, S. Gåseidnes, R. Sirevåg, B. Synatad, B. van der Burg, Rational engineering of enzyme stability, J. Biotechnol. 113 (2004) 105–120.
[19] S. Radestock, H. Gohlke, Exploiting the link between protein rigidity and thermostability for data-driven protein engineering, Eng. Life Sci. 8 (2008) 507–522.
[20] A.J. Rader, B.M. Hespenheide, L.A. Kuhn, M.F. Thorpe, Protein unfolding: rigidity lost, Proc. Natl. Acad. Sci. U.S.A. 99 (2002) 3540–3545.